Catena 247 (2024) 108442

Contents lists available at ScienceDirect

Catena

journal homepage: www.elsevier.com/locate/catena

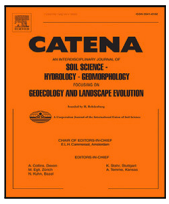

Unravelling the spatial structure of regular dryland vegetation patterns

Karl Kästner [a,*], Roeland C. van de Vijsel [b], Daniel Caviedes-Voullième [c,d], Nanu T. Frechen [a], Christoph Hinz [a]

[a] Hydrology, Brandenburg University of Technology Cottbus–Senftenberg, 03046 Cottbus, Germany
[b] Hydrology and Environmental Hydraulics Group, Wageningen University, 6708 PB Wageningen, The Netherlands
[c] Institute of Bio- and Geosciences: Agrosphere (IGB-3), Forschungszentrum Jülich, 52428 Jülich, Germany
[d] Simulation and Data Lab Terrestrial Systems, Jülich Supercomputing Centre (JSC), 52425 Jülich, Germany

ARTICLE INFO

Dataset link: https://github.com/karlkastner/environmental-spatial-patterns-periodicity-test, https://zenodo.org/records/13695204, https://www.riverdolphin.xyz/vegetation-patterns.html

Keywords:
Self-organization
Arid vegetation
Stochastic processes
Turing pattern
Spectral analysis

ABSTRACT

Many resource-limited ecosystems exhibit spatial patterns where patches of biomass alternate with bare ground. Patterns can enhance ecosystem functioning and resilience, depending on their spatial structure. Particularly conspicuous are regular patterns, where patches are of similar size and spaced in similar intervals. The spatial structure of regular patterns is often described to be periodic. This has been corroborated by statistical testing of natural patterns and generation of periodic patterns with deterministic reaction–diffusion models. Yet, natural regular patterns appear conspicuously erratic compared to periodic patterns. So far, this has been attributed to perturbations by noise, varying patch size and spacing. First, we illustrate by means of an example that the spatial structure of regular vegetation patterns cannot be reproduced by perturbing periodic patterns. We then compile a large dataset of regular dryland patterns and find that their spatial structure systematically differs from periodic patterns. We further reveal that previous studies testing for periodicity overlook two aspects which dramatically inflate the number of false positives and result in the misclassification of patterns as periodic. We amend the test procedure by accounting for both aspects, finding that regular natural patterns have no significant periodic components. Lastly, we demonstrate that stochastic processes can generate regular patterns with similar visual appearance, spatial structure and frequency spectra as natural regular patterns. We conclude that new methods are required for quantifying the regularity of spatial patterns beyond a binary classification and to further investigate the difference between natural and model generated patterns.

1. Introduction

Many physical, chemical and biological systems alternate in space or time between different local states (Rietkerk and van de Koppel, 2008; Kondo and Miura, 2010; Goehring, 2013). Fascinating spatial patterns (Fig. 1a, b) consisting of patches of high biomass alternating with bare ground are found in many resource-limited ecosystems (Rietkerk and van de Koppel, 2008). The emergence or change of such patterns may indicate the deterioration and imminent catastrophic shifts in ecosystems (Kéfi et al., 2007; Kefi et al., 2014), as they are linked to environmental harshness such as aridity (Rietkerk et al., 2002). Moreover, patterns can also increase ecosystem productivity (Pringle et al., 2010), water use efficiency (Boer and Puigdefábregas, 2005) and resilience (Borgogno et al., 2009). The relation between a pattern's characteristics and its effect on resilience is therefore complicated (Pascual and Guichard, 2005). Ecosystem resilience depends on the particular properties of its pattern, such as its characteristic wavelength (Yizhaq et al., 2005; Siero et al., 2015) or structure (Weerman et al., 2012; Roitberg and Shoshany, 2017; Bastiaansen et al., 2020; Rietkerk et al., 2021). A thorough understanding of a pattern's structure and its relation to ecosystem functions is thus paramount for assessing ecosystem health and susceptibility to environmental pressure.

Whenever something alternates in a regular manner, it is reasonable to consider the presence of periodicities. Identifying periodicities can reveal deterministic processes and thus facilitate a better understanding of the physical system at hand. An example are the ocean tides driven by the perpetual movement of the celestial bodies (Doodson, 1921; Parker, 2007). Periodic patterns can also be spatial, for example in plantations where individual trees are aligned with respect to a common reference (Fig. 1c_i, d_i). Conspicuously regular spatial patterns are also found in ecosystems with scale-dependent feedbacks such as close-range facilitation and far-range competition (Fig. 1a_i, b_i). They are therefore described as periodic, i.e. to repeat at their characteristic wavelength corresponding to the distance between neighbouring patches (Couteron and Lejeune, 2001; Couteron et al., 2014; Okayasu

* Corresponding author.
E-mail address: kastner.karl@gmail.com (K. Kästner).

https://doi.org/10.1016/j.catena.2024.108442
Received 19 February 2024; Received in revised form 18 September 2024; Accepted 30 September 2024
Available online 16 November 2024

and Aizawa, 2001; Rietkerk et al., 2002; Lejeune et al., 2004; Deblauwe et al., 2008, 2011, 2012; Borgogno et al., 2009; von Hardenberg et al., 2010; Kletter et al., 2012; Penny et al., 2013; Zelnik et al., 2013, 2015; Barbier et al., 2014a,b; Meron, 2015; Getzin et al., 2015; Messaoudi et al., 2020; Tlidi et al., 2020; Wang et al., 2023; Moreno-de Las Heras et al., 2011; Sankaran et al., 2019; Kefi et al., 2014; Siteur et al., 2023; Mander et al., 2017; Maestre et al., 2016; Sheffer et al., 2013). Natural patterns can be randomly perturbed by exogenous factors so that they do not exactly repeat. Such perturbations have been described by added noise, varying patch size and varying distance between patches (Couteron, 2002; Scheffer et al., 2009; Kéfi et al., 2010a; Barbier et al., 2010; Moreno-de Las Heras et al., 2011; Weerman et al., 2012; Sheffer et al., 2013; Kefi et al., 2014; Meron, 2015; Mander et al., 2017; Sankaran et al., 2019; Bastiaansen et al., 2020; Siteur et al., 2023). Perturbed periodic patterns still have a periodic structure, which can be revealed by their spatial autocorrelation or frequency spectra, as in the case of plantations (Fig. 1c_{ii}, d_{ii}).

However, it is reasonable to consider that the process of pattern formation is perturbed as well, in which case it resembles a stochastic process. This means that the biophysical feedbacks are randomly perturbed, not that they are absent (van Kampen, 1976). Patterns which form through stochastic processes can still be regular, i.e. appear similar to themselves when shifted by the distance of one characteristic wavelength, but the perturbations prevent the crystallization of a periodic structure. Many stochastic physical processes alternate in a regular fashion and create patterns which appear similar to themselves when shifted in time or space by a distance corresponding to their characteristic wavelength. Examples are the climatic Daansgard-Oeschger warming events (Ditlevsen et al., 2005) the El Niño - Southern Oscillation (ENSO) (Stone et al., 1998; An et al., 2020), or the interval at which hens lay eggs (Johnston and Gous, 2007). Both periodic patterns and regular stochastic patterns appear similar to themself when shifted by a multiple of their characteristic wavelength. The fundamental difference between periodic and a regular stochastic patterns is that periodic oscillations remain indefinitely correlated in time or globally in space, while stochastic oscillations decorrelate. The autocorrelation of periodic patterns thus oscillates with constant amplitude, as in the case of tidal oscillations, while the autocorrelation of regular stochastic patterns oscillates with decaying amplitude, as in the case of ENSO. As the amplitude of the autocorrelation of regular environmental spatial patterns decays (Fig. 1a_{ii}, b_{ii}), it seems plausible that they form through stochastic processes.

This observation contradicts the general perception that the spatial structure of environmental spatial patterns is periodic. Previous studies supported this by analysing regular environmental spatial patterns with methods suitable for finding periodicities hidden in a noisy background (Couteron and Lejeune, 2001; Couteron, 2001; Couteron et al., 2006; van de Koppel et al., 2005; Kefi et al., 2014). Motivated by our observation, we investigate whether the spatial structure of regular vegetation patterns is periodic, and if it can be reproduced by stochastic processes instead.

Patterns are usually classified based on a statistical test, as a visual inspection of their correlation structure or frequency spectrum is subjective. For this, a pattern is first transformed into the frequency domain. Then, it is tested if the frequency component with the largest magnitude significantly exceeds the value expected for noise. These tests led to the conclusion that regular environmental patterns are periodic. However, previous studies have missed out two important aspects which has inflated the number of false positives (Type-I errors) and resulted in the misclassification of regular environmental spatial patterns as periodic: first, previous studies test the frequency component with the largest magnitude against a critical value applicable for testing a single a-priori known frequency component. However, testing the frequency component with the largest magnitude is equivalent to testing all frequency components and rejecting the null hypothesis when the magnitude of any component exceeds the critical value. The probability that the magnitude of any frequency component exceeds the critical value is much higher than that the magnitude of a single a-priori known frequency component exceeds it, as it consists of multiple comparisons. The critical value has to be raised so that the probability of misclassifying a random pattern as periodic (Type-I error) is in accordance with the confidence level (Thomas, 1973). Second, previous studies assumed white noise as the null model, which has a flat spectral density, and to a limited extent to coloured noise, which has no local maxima (Barbier et al., 2010). Noise is the stochastic, i.e. non-deterministic component of an image. The spectral density of stochastic processes is not necessarily flat. Environmental spatial patterns typically have a strong stochastic component with a lobed spectral density i.e. the shape of its density is similar to that of unimodal probability density, which has a local maxima and slowly tapers off to either side (Fig. 1a_{iii}, b_{iii}). As the magnitude of frequency components of noise with lobed spectral density exceeds the expected magnitude of noise with a flat density, testing against a flat density thus inflates the number of Type-I errors in such a case. This can be avoided by testing against the lobed density. Here, we revise the statistical test and apply it to a large novel dataset of environmental spatial patterns, to determine if regular environmental spatial patterns are periodic or not.

This manuscript is structured as follows: In Sections 1.1 and 1.2, we clarify the definitions of periodic patterns forming through deterministic processes and regular patterns forming through stochastic processes. We illustrate their spatial correlation structure and frequency spectra, and demonstrate that the structure and spectra of natural regular patterns is distinct from that of periodic patterns, but similar to that of regular patterns originating from stochastic processes. In Section 2, we introduce a statistical test for periodicity, accounting both for the effect of multiple comparisons and that the stochastic component of a pattern can have a lobed spectrum. In Section 3, we apply the test to a large novel dataset of regular patterns, finding that the patterns are not periodic. In Section 4 we discuss the implications of our findings.

1.1. Spatial structure of periodic and regular patterns

Regular environmental spatial patterns are often interchangeably described as being regular and periodic, with the terms not being clearly distinguished. We therefore clarify the differences first. In the idealized case of patterns with infinite spatial extent, the spatial structure is determined by the autocorrelation function R, which shows the degree of similarity of a pattern with a copy of itself shifted in space. Patterns with finite spatial extent can be interpreted as being cropped from a pattern with infinite extent, and the autocorrelation function can be estimated from it, c.f. supplement, section 4.2. This estimate is called the correlogram $\hat{R}$. The correlogram systematically deviates from the autocorrelation function due to the finite spatial extent, which complicates its analysis, as elaborated at the end of the section.

1.1.1. Periodic patterns

A one-dimensional periodic pattern repeats, i.e. is identical to itself when shifted by a particular distance. The autocorrelation function consequently periodically oscillates as well, with the value 1 at multiples of this distance. When the pattern consists of a dominant frequency component with wavenumber k_c and harmonic components at integer multiples of this wavenumber, then the distance at which the pattern repeats is the characteristic wavelength $\lambda_c = 2\pi/k_c$. In two dimensions, a periodic pattern repeats, i.e. is identical to itself, when translated into any direction with rational angle. The distance at which it repeats depends both on the direction and the frequency components. The autocorrelation function consequently periodically oscillates with value 1 in any direction, where the distance depends on the direction. Periodic axis-symmetric patterns, such as striped patterns, can therefore be cut in identical stripes, and radially-symmetric patterns, such as hexagonal patterns, can be tessellated into identical tiles (Fig. 2a_i, b_i).

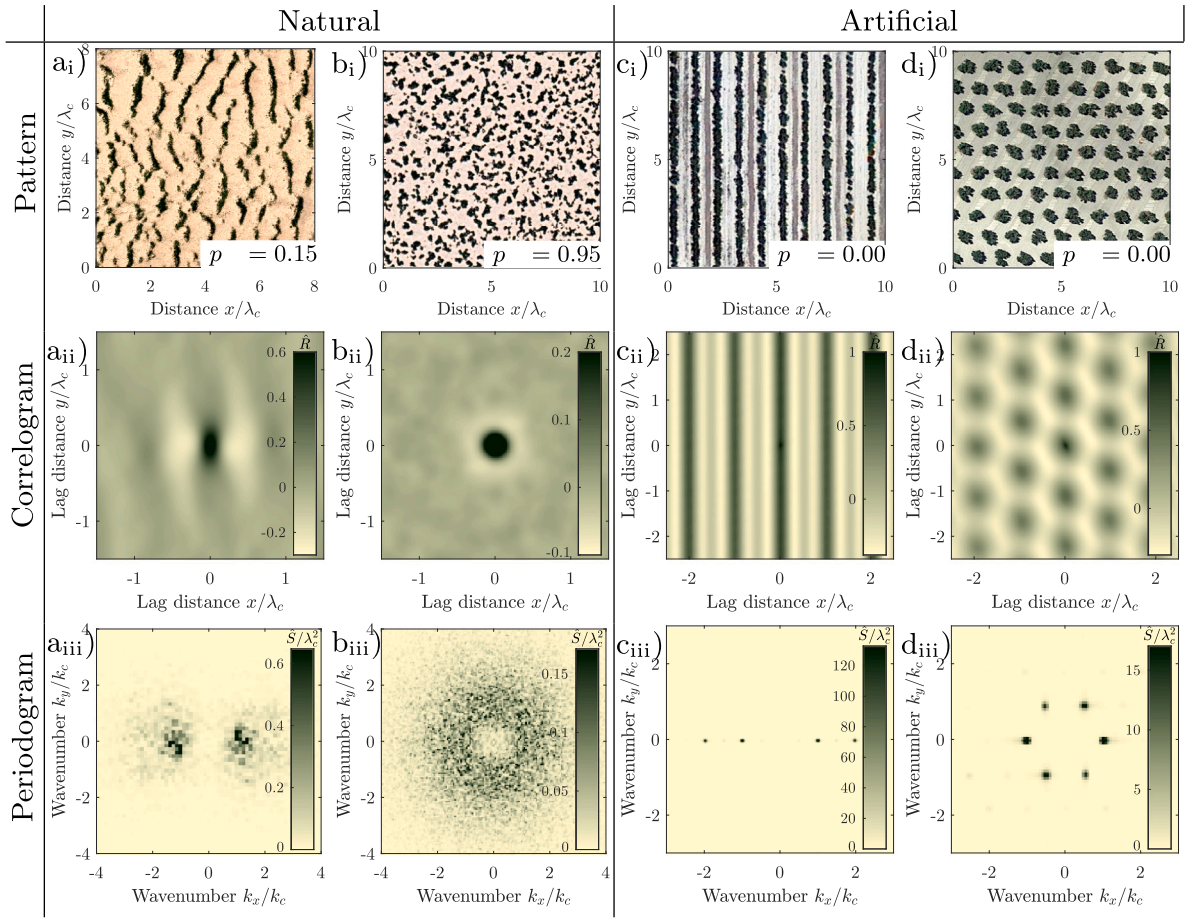

Fig. 1. Regular natural and periodic artificial vegetation patterns with their correlograms and periodograms. (a) Natural anisotropic pattern in Chihuahua, Mexico (107.15° W 31.34° N). Characteristic wavelength λ_c = 88 m, relative image size L/λ_c = 9. (b) Natural isotropic pattern in Coahuila, Mexico (103.14° W 27.66° N). Characteristic wavelength λ_c= 32 m, relative size of uncropped image L/λ_c = 21. (c) Artificial striped pattern of a plantation in Granada, Spain (2.69 W°, 37.57 ° N). Characteristic wavelength λ_c = 7.5 m, relative size uncropped image L/λ_c = 32. (d) Artificial hexagonal pattern of a plantation in Seville, Spain (5.36° W 37.40° N) Characteristic wavelength λ_c = 14 m, relative size of uncropped image L/λ_c = 15. Large images have been cropped for display to a spatial extent with a side length of 10 wavelengths. Satellite images by Maxar Technologies and Google (2023).

Periodic patterns can form in excitable deterministic systems (Meron, 1992; Murray, 2002) but cannot be expected to be immaculate in nature as they are likely perturbed by spatial noise, randomly varying patch size, spacing or shape. While such perturbations add random, i.e. stochastic components, the pattern retains a periodic spatial structure as long the individual patches remain aligned with respect to a global reference. The autocorrelation of a perturbed periodic pattern still oscillates with constant amplitude, but the amplitude is reduced globally by a constant factor due to the presence of the stochastic components. Trees in plantations are often periodic as they are aligned with respect to a global reference (Fig. 1c_i, d_i). The underlying spatial structure remains periodic even if individual trees are displaced, deviate in size or are removed. The autocorrelation of both the natural striped and spotted pattern oscillates, identifying them as regular patterns (Fig. 1a_{ii}, b_{ii}). However, the oscillation decays rapidly, which indicates that they do not have a periodic spatial structure. The natural spotted pattern also does not have a hexagonal structure, i.e. patches are not aligned along axes of symmetry as in the case of the periodic pattern. In contrast, the periodic spatial structure is clearly visible in the correlograms of the plantation patterns (Fig. 1c_{ii}, d_{ii}). The absence of a periodic structure cannot merely be explained by a perturbation of a periodic pattern. We demonstrate this by synthesizing a strongly perturbed periodic pattern. Despite the perturbations, the periodic structure is retained (Fig. 2a_i, b_i).

1.1.2. Regular patterns

While patterns are often described as regular, regularity itself is often not clearly defined. Weerman et al. (2010) identify a pattern as regular when its autocorrelation has a local maximum at a lag distance separate from zero. Based on this, we introduce the following definition: a pattern is regular when the autocorrelation oscillates in at least one direction. The amplitude of the oscillation may decay. A regular pattern is thus similar, but not identical, to itself when shifted by a distance equal to its characteristic wavelength λ_c. The further a pattern is shifted, the more the similarity decreases, according to the decay of the autocorrelation. The patches are only aligned with respect to their neighbours but not with respect to a global reference. The size, shape, orientation and distance between patches intrinsically varies. The patches are only locally aligned with respect to their neighbours but not with respect to a global reference. A regular pattern is not symmetric and cannot be cut into identical stripes or tiles.

Regular patterns can form through stochastic processes. A stochastic process is a process where a variable or parameter is randomly perturbed by noise in time or space. Stochasticity hence does not imply the absence or irrelevance of biophysical feedbacks, only its perturbation. Stochastic patterns can be synthesized by introducing spatial correlation into spatial noise. This can be facilitated by convolving uncorrelated noise with the autocorrelation function of a stochastic process, c.f. supplement sections 3.10 and 4.9. Suitable choices for the autocorrelation functions are characteristic functions of common two-parametric unimodal probability distributions, where the combination

of the two parameters determines the length scale and degree of regularity. It is unnecessary to add noise when synthesizing a random regular pattern. We find that the autocorrelations of the natural patterns in our example appear quite similar to that of synthesized random regular patterns (Fig. 2c$_i$, d$_i$), i.e. they oscillate with a rapidly decaying amplitude. The synthesized regular spotted pattern has furthermore a similar annular structure as the natural regular pattern, in contrast to the hexagonal structure of the periodic pattern. Stochastic processes can also generate irregular patterns. The autocorrelation of irregular patterns thus decays without oscillating (Pielou, 1964).

Despite its intuitive definition, the correlogram is not ideal for a direct statistical analysis of spatial structures as it has undesirable statistical properties: The oscillation of the correlogram of a periodic pattern spuriously decays when it is cropped to a spatial extent that is not a multiple of its characteristic wavelength, c.f. supplement, section 4.2. The oscillation also spuriously decays when the correlogram is transformed into radial coordinates for separating radial and angular components of isotropic patterns, c.f. supplement 4.4. Harmonic frequency components can further complicate the identification of the characteristic wavelength.

It is therefore desirable to analyse patterns with superior methods than the correlogram. The distribution of patch size and patch spacing is frequently employed for the studying spatial structures of environmental spatial patterns (Kéfi et al., 2007; Bastiaansen et al., 2020). However, they are unsuitable to determine if the spatial structure is periodic or not as patch size and spacing can vary in regular patterns irrespectively if their spatial structure is periodic or not, as shown above. We therefore base our analysis on the frequency spectrum, i.e. on the periodogram $\hat{S}$, as it does not suffer from the same shortcomings of the autocorrelation, and is suitable for distinguishing regular stochastic from periodic patterns.

1.2. Frequency spectra of regular patterns

The spectral density S of a pattern shows the fraction of the spatial variance contributed by each frequency component, c.f. supplement, section 3.1. It contains the same information as the autocorrelation function, in particular the information if a pattern spatial structure is periodic or not, as both are the Fourier transform of each other. The discrete analogue of the spectral density is the periodogram $\hat{S}$, which can be readily computed from an aerial image of a pattern. For stochastic components, the periodogram values are random. Their mean and variance is proportional to the spectral density. The periodogram does not consistently estimate the spectral density (Parzen, 1957), as its variance does not decrease with the image size or resolution. However, the spectral density can be consistently estimated by smoothing the periodogram, c.f. supplement section 3.1.

1.2.1. Periodic patterns

The frequency spectrum of a periodic pattern is discrete as it consists of well-separated narrow and high peaks at wavenumbers distinct from zero (Jenkins and Priestley, 1957). The peaks correspond to the frequency components of the pattern. The distance of the origin of each peak determines the wavenumber and the angle its direction of each frequency component. The highest peak determines the dominant frequency component and characteristic wavenumber $k_c = 2\pi/\lambda_c$. As the pattern is real valued, each frequency component has two peaks of identical height mirrored with respect to the point of origin, i.e. separated by 180°. Axis-symmetric patterns, such as striped patterns, typically have a pair of peaks with the radial wavenumber $\pm k_c$. Spotted patterns with hexagonal structure have six peaks with the radial wavenumber k_c separated by 60° (Ouyang and Swinney, 1991). Harmonic frequency components result in smaller peaks which are well separated from the main frequency components. When a pattern is cropped to a finite spatial extent and the spectrum is normalized to integrate to 1, then the magnitude of the peaks S_p are of the order L^2 for two-dimensional patterns in the square domain with area L^2, c.f. supplement section 3.6.

Random perturbations such as varying patch size, spacing and spatial noise introduce non-periodic frequency components. Noise typically consists of many frequency components so that the magnitude of the individual frequency components is small, in particular for white noise the magnitude S_w is L^2/n^2 ((Kovačević and Djurović, 2008, Chapter 2.5)), where n is the number of independent pixels in the image. When periodic frequency components contribute the fraction q to the total spatial variation and the noise the fraction $1-q$, then the peak-to-noise ratio is $S_p/S_w = n^2\,q/(1-q)$. The peak-to-noise ratio is therefore high even when the spectral energy of the periodic component is distributed over several components and the pattern is considerably perturbed by noise, as the number of independent pixels n^2 is typically large. Averaging the periodogram along one dimension and normalizing its area to 1 results in peaks with magnitude L, noise with magnitude L/n and peak-to-noise ratio of $n\,q/(1-q)$. The frequency spectra of the plantation patterns appear quite similar to the spectra of periodic patterns 1c$_{iii}$, d$_{iii}$, with well-separated peaks of the expected magnitude. However, the frequency spectra of the natural regular patterns do not appear similar to that of periodic patterns, as their spectral components are scattered and of lower magnitude (Fig. 1a$_{iii}$, b$_{iii}$).

1.2.2. Regular patterns

A pattern is regular when its spectral density is lobed, where the maximum of the lobe occurs at the characteristic wavenumber $k_c = 2\pi/\lambda_c$, and is well separated from zero ($k_c > 0$). This corresponds to our definition in Section 1.1.2, where we define regular patterns as patterns where the autocorrelation oscillates with decaying amplitude. This can be shown by determining the spectral density from the autocorrelation via the Fourier transform, c.f. supplement, section 4.1. Consequently, the frequency components of regular stochastic patterns are randomly scattered in a region around the characteristic wavenumber k_c (Fig. 2c$_{iii}$, d$_{iii}$) instead of being concentrated in peaks. For anisotropic patterns, e.g. striped patterns, the frequency components are scattered in two regions with radial wavenumber k_c separated by 180° and for isotropic, e.g. spotted, patterns in an annular region with radius k_c. The periodogram of isotropic stochastic patterns thus does not have axes of preferential patch alignment. The magnitude of frequency components near the characteristic wavenumber is typically much smaller than that of a periodic pattern L^2 but much larger than that of white noise $(L/n)^2$. In contrast to periodic patterns, the magnitude also does not depend on the spatial extent of the pattern. When the periodogram is smoothed to reveal the underlying density, then the density appears to be lobed, not peaked, i.e. it decays gradually with increasing distance from the local maximum at the characteristic wavenumber. The frequency spectrum of a regular stochastic pattern can be synthesized as the product of an unimodal, i.e. lobed, probability density and uncorrelated noise, or conversely by taking the Fourier transform of a pattern generated by convolving uncorrelated noise with the characteristic function of the probability distribution, c.f. supplement section 4.1. We find that the frequency spectra of the natural patterns (Fig. 1a$_{iii}$, b$_{iii}$) are quite similar to the spectra of regular random patterns synthesized in this manner (Fig. 2c$_{iii}$, d$_{iii}$). We note that irregular patterns have a lobed spectral density where the maximum of the lobe occurs at the zero wavenumber (Pielou, 1964). so that the frequency components of the periodogram are randomly scattered around the origin.

1.3. Relation between periodic and regular patterns

Periodic and irregular patterns are limit cases of regular patterns. A pattern is periodic, when the autocorrelation oscillates with constant amplitude, and correspondingly, when its spectral density consists of peaks well separated from the zero wavenumber. A pattern is irregular,

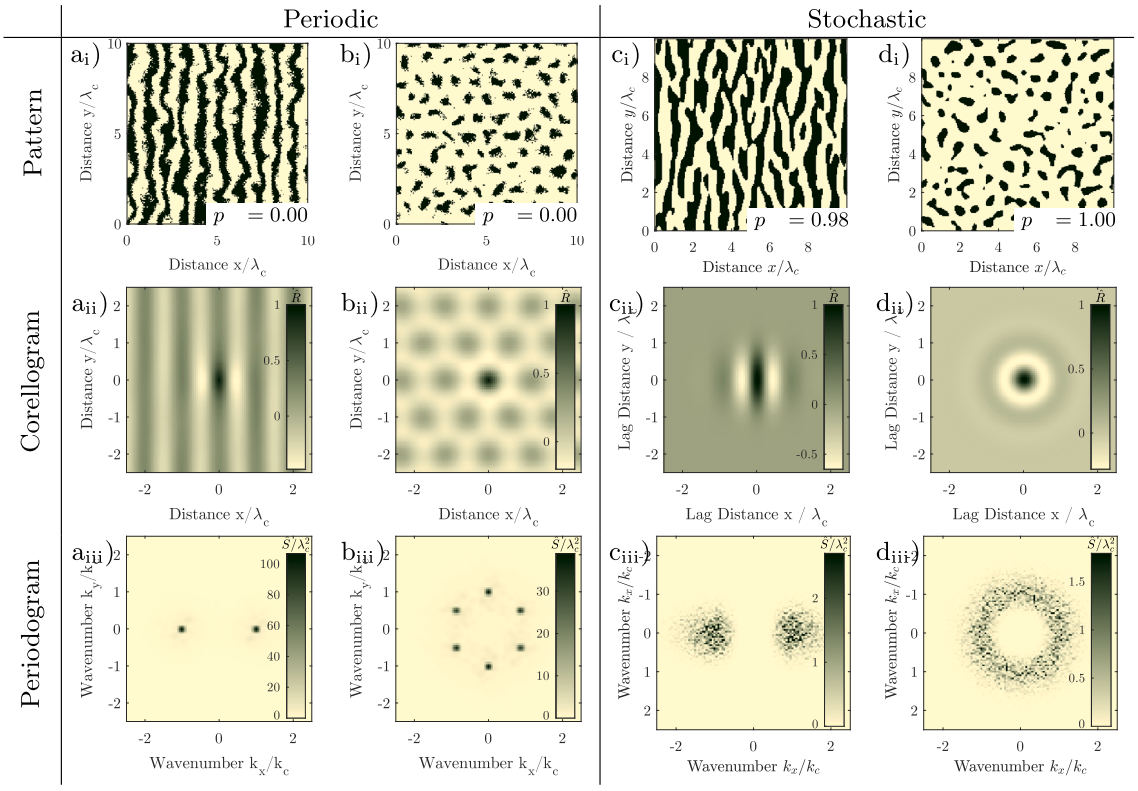

Fig. 2. (a_i, b_i) Synthetic periodic patterns perturbed by added spatial noise, varying patch size and spacing. (a_{ii}, b_{ii}) The correlogram reveals the periodic, i.e. repeating structure, through its oscillation at the characteristic wavelength. (a_{iii}, b_{iii}) The spectral energy is concentrated in well-separated peaks at the characteristic wavenumber. (c_i, d_i) Synthetic regular random patterns generated by a stochastic process following a gamma-distribution. (c_{ii}, d_{ii}) The correlogram oscillates but the oscillation decays. (c_{iii}, d_{iii}) The spectral energy is scattered in a region around the characteristic wavenumber. Note the similarity between the natural regular patterns in Fig. 1 and the synthesized regular random patterns and dissimilarity with the synthesized periodic patterns. All patterns were generated in a square domain with side length $L = 20\lambda_c$, where λ_c is the characteristic wavelength of the pattern, and pixel side length $\Delta x = \lambda_c/20$, resulting in comparable spatial and spectral resolution. For display, the patterns have been thresholded and cropped to a side length of 10 λ_c.

when the autocorrelation decays gradually, i.e. does not oscillate, and correspondingly, when the lobe of the spectral density is centred at the origin. A periodic pattern is therefore regular, but a regular pattern is not necessarily periodic. Similarly, deterministic processes are a limit case of stochastic processes where the random perturbations are negligible. Whether a pattern is periodic or not is therefore relevant for the pattern formation. When regular environmental spatial patterns have a periodic spatial structure, then the structure can be well reproduced with deterministic models and the variation of patch properties can be considered as extraneous. However, if the spatial structure is not periodic, then the influence of stochastic processes, i.e. noise, on the pattern formation is not negligible, and the variation of patch properties is intrinsic.

Both the autocorrelation structure and frequency spectrum of the two regular natural patterns in our example indicate that they are regular, but nor periodic. To substantiate this finding, we revisit statistical tests for periodicity in the following section.

2. Testing for periodicity

The dichotomous questions if the spatial structure of a pattern is periodic or not can be decided with a statistical test. Periodicity is typically shown by refuting the null hypothesis that the magnitude of a frequency component of the periodogram $\hat{S}$ is significantly larger than the value expected for spatial noise with spectral density S_s:

$$\max\left(\frac{\hat{S}}{S_s}\right) > \frac{1}{2}\left(\chi_2^2\right)^{-1}(1-\alpha) = -\ln\alpha. \tag{1}$$

c.f. Li (2013), where χ_2^2 is the Chi-squared distribution with two-degrees of freedom. We interpret the spectral density as a probability density and the autocorrelation function correspondingly as its characteristic function. For this, we normalize the volume of the periodogram $\hat{S}$ and consequently of the density S to 1. This does not affect the test as the normalization cancels in the ratio $\hat{S}/S_s$, though it facilitates comparing the spectrum with common probability densities. α is the confidence level for accepting the frequency component as being periodic. In a set of patterns conforming to the null level model, i.e. consisting entirely of spatial noise, the expected fraction of patterns with significant frequency components (Type-I Error), is identical to the confidence level α.

When the noise is white, then the spectral density S_s is flat, and for a pattern sampled along a transect (d=1) or square domain (d=2) with side length L at n-grid points spaced in equal distance along each dimension the density is, c.f. supplement section 3.7:

$$S_w = \left(\frac{L}{n}\right)^d. \tag{2}$$

In this case, the narrow and isolated peaks of the discrete spectra of the periodic pattern rise high above the flat noise spectrum. The test only assesses if a frequency component exceeds the threshold in Eq. (1). It does not assess how well a periodic function describes the frequency spectrum of a pattern. This can be assessed by the fraction of the spatial variance contributed by the significant frequency components.

Periodicity could also be tested by other means, for example based on the autocorrelation. A test of the autocorrelation will lead to the similar result as a test of the periodogram, as both are the Fourier transform of each other, and thus contain identical information, c.f. supplement section 4.1. We conduct our analysis based on the periodogram, due to its preferential statistical properties.

2.0.1. Fraction of patterns with periodic frequency components

A test only assesses if a pattern contains significant components. It cannot determine if a significant frequency component originates from a deterministic process and is periodic, or if it stems from a stochastic process and just exceeds the critical value by chance. While it is not possible to determine the origin of a significant frequency component for a single pattern, it is possible to determine the fraction of patterns with periodic components stemming from deterministic processes by testing a large number of patterns. When the periodic and stochastic parts are uncorrelated, then the total fraction of patterns with significant frequency components c is:

$$c = a + b - a \cdot b, \tag{3}$$

where a is the fraction of patterns where a frequency component of the stochastic part is significant, b is the fraction of patterns where a periodic frequency component stemming from a deterministic process is significant, and $a \cdot b$ is the fraction of patterns with both significant stochastic and deterministic frequency components. The fraction of patterns with significant deterministic frequency components is thus:

$$b = \frac{c - a}{1 - a}. \tag{4}$$

The expected fraction of patterns with significant stochastic components is $E[a] = P(p < \alpha) = \alpha$ so that $E[b] = (c - \alpha)/(1 - \alpha)$. For the arbitrary choice $\alpha = 0.05$, 5% of all stochastic patterns have significant frequency components. As α is small, $b \approx c - \alpha$, and comparing the fraction of patterns with significant frequency components c against the confidence level α will indicate the fraction of patterns containing periodic components originating from deterministic processes. As the dataset is finite, the number of stochastic patterns with significant frequency components varies randomly around the expected value α. The standard error $\mathrm{se}(a)$ is $\mathrm{se}(a) = \sqrt{\alpha(1-\alpha)/n}$, when n patterns are tested. For drawing a significant conclusion, a sufficiently large number of patterns, say at least 100, has to be tested.

2.0.2. Accounting for multiple comparisons

Eq. (1) is for testing a single predetermined frequency component for significance. It is suitable for testing for the presence of a spectral line of a particular chemical element in the light of distant stars, or the presence of a particular tidal constituent in a water level record. In the case of a natural pattern, the dominant frequency component is not known a priori, but determined from the data. The test thus consists of multiple comparisons, as the null hypothesis is only not rejected, i.e. the pattern is classified as having no periodic frequency component, when all periodogram values fall below the threshold α.

Multiple comparisons have to be accounted for by reducing the value of the confidence level α with the Bonferroni correction (Li, 2013). This in turn results in a higher critical value for a pattern to be classified as periodic. When n_t periodogram bins are tested in total, then the modified value α_{n_t} to be used for the test is:

$$\alpha_n = 1 - (1 - \alpha_1)^{1/n_t} \approx \frac{\alpha_1}{n_t}, \tag{5}$$

where α_1 is the desired confidence level. Since the periodogram is symmetric, only half the frequency components have to be tested so that $n_t = n/2$ for transects and $n_t = n^2/2$ for square domains. As n is typically large, $\alpha_n \ll \alpha_1$ so that most stochastic patterns will be misclassified as periodic when α_1 instead of α_n is used when testing, c.f. Fig. 3.

The Bonferroni correction is essential for a periodicity test. It is therefore usually applied in statistical textbooks without being explicitly mentioned (Percival et al., 1993, ch. 10.9). It is also not mentioned in previous studies where environmental spatial patterns have been tested (Couteron, 2001; Couteron et al., 2006). However, it is also not applied, as is evident from the example in Renshaw and Ford (1984), on which the later publications are based on: For a pattern sampled on a square 32×32 grid and a confidence level of $\alpha = 0.05$, they use the critical value of $0.0059 = \left(\chi^2_2\right)^{-1}(1 - 0.05)/32^2$ relative to the total variance. The spatial extent of the pattern L is not required for testing, as the normalization cancels from the tested ratio, c.f. equation (1). A frequency component is significant when its magnitude exceeds the critical value. 5% of all frequency components of white noise exceed this critical value, and consequently nearly all patterns consisting of white noise are misclassified as periodic, as each pattern has $32^2/2 = 512$ independent frequency components ($1 - (1 - 0.05)^{512} \approx 1$). The correct critical value is $0.018 = \left(\chi^2_2\right)^{-1}(1 - 0.05/512)/32^2$ for which only 5% of all patterns consisting of white noise are misclassified ($1 - (1 - (0.05/512))^{512} \approx 0.05$), in agreement with the confidence level α.

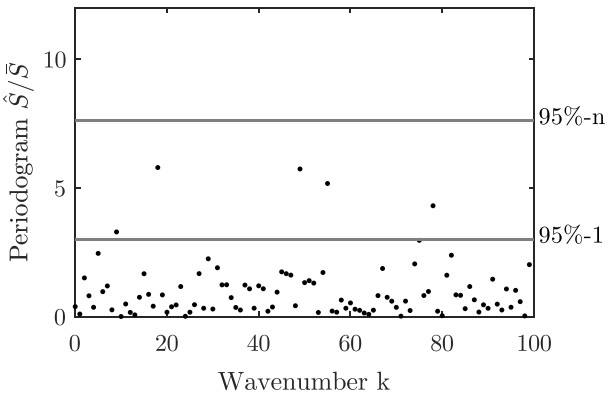

Fig. 3. Periodogram of a one-dimensional pattern consisting of white noise. The line 95%-1 indicates the level exceeded by 5% of all frequency bins, testing against this level misclassifies almost all patterns as periodic. The line 95%-n indicates the corrected level exceeded by the maximum value of all frequency bins within 5% of all patterns. None of the frequency components in the example exceeds the corrected level. With the Bonferroni correction, the pattern is thus correctly classified as not periodic.

2.0.3. Arbitrary noise spectra

Another caveat when testing for periodicity is that it requires the spectral density of the spatial noise to be known for the null model. Previous studies assume that the noise is uncorrelated (white noise), which corresponds to a flat spectral density (equation (2)), (Mugglestone and Renshaw, 1998; Couteron, 2001, 2002; Couteron et al., 2006; Kefi et al., 2014), or coloured noise (Barbier et al., 2010) which have no local maxima. Noise results from stochastic processes and can be superimposed to a pattern, such as photon noise stemming from the image acquisition, but it can also be inherent to a pattern when it results from stochastic processes in the pattern formation. Photon noise is white but its magnitude is usually negligible in high-quality images. In contrast, the spectrum of a typical natural vegetation pattern has a strong stochastic component in the form of a wide lobe (Fig. 1a, b). Testing the periodogram of a pattern with a lobed spectrum against the flat spectrum of white noise strongly inflates the number of false positives.

Consequently, the periodogram has to be tested against the lobed spectrum of the noise. The spectral density of the noise is not known, though it can be estimated, for example by fitting a particular parametric density model. To avoid the complications that arise from selecting and fitting an appropriate density model, we estimate the density non-parametrically, by suppressing the noise in the periodogram by smoothing. Replacing the density S_s with its estimate $\bar{S}$ changes the test statistics, as the ratio $\hat{S}/\bar{S}$ is not χ^2-distributed. When the smoothing window consists of m bins of equal weight, the ratio is Beta-distributed (c.f. supplement section 6.1):

$$\frac{\hat{S}}{\bar{S}} \sim m\, B_{1,m-1}. \tag{6}$$

This approaches the χ^2-distribution for large m. The p value of the test is thus $\left(1 - B_{1,m-1}\left(\hat{S}/\left(m\,\bar{S}\right)\right)\right)^n$, where $B_{1,m-1}$ is the cumulative Beta-distribution and m the total number of frequency bins of the smoothing

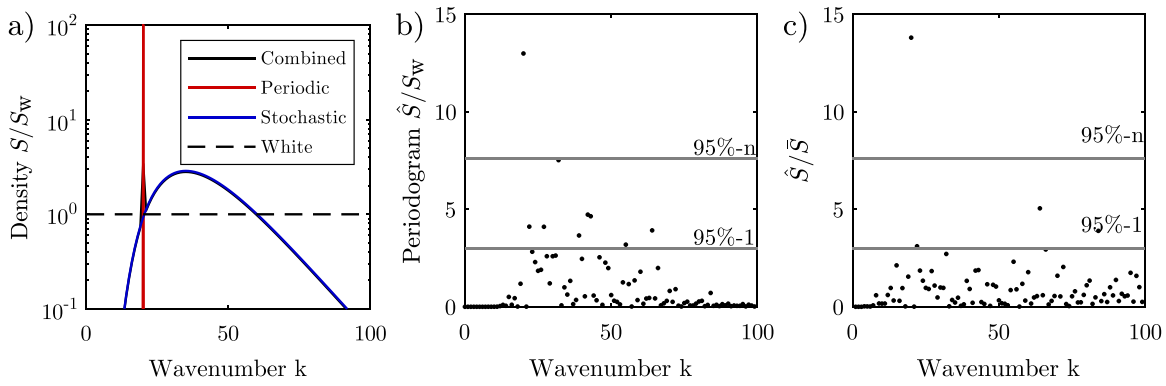

Fig. 4. (a) Spectral density S (black) of a one-dimensional pattern consisting of a periodic component with peaked density and a stochastic component (spatial noise) with lobed density. The density is normalized by the density of white noise S_w. The pattern is artificial and has been synthesized for illustration. (b) Periodogram $\hat{S}$ of the pattern. The magnitude expected for white noise is not only exceeded by the frequency component associated with the periodic component, but also where the density of the stochastic component is high. (c) Periodogram of the pattern normalized the estimated spectral density of the stochastic component $\bar{S}$, only the periodic component remains significant. Horizontal lines indicate confidence levels as in Fig. 3.

window. Here, we smooth the periodogram within a circular window containing m bins with equal weights. Testing against the estimated density brings the number of false positives (Type-I errors) close to the expected value (Fig. 4). The maximum $\hat{S}/\bar{S}$ occurs at the wavenumber of the periodic frequency component with largest magnitude, if such a component is present. Otherwise, the maximum $\hat{S}/\bar{S}$ occurs at a random wavenumber, i.e. not necessarily at the wavenumber where the spectral density of the stochastic part S_s reaches its maximum, because the normalization with $\bar{S}$ flattens the spectrum.

We note that it is unnecessary to separate the deterministic from the stochastic part of the spectrum for the test. We test the ratios $\hat{S}/\bar{S}$ of the periodogram $\hat{S}$ with the estimated density $\bar{S}$ of the total spectrum. S_s potentially contains smoothed periodic components in addition to the noise. This avoids a circular dependency on the determination of periodic components. It does not considerably reduce the power of the test as long as periodic frequency components are isolated. However, the test is biased for highly regular stochastic patterns as the lobe of their spectral density is narrow. Estimating the density by smoothing results in an underestimation of its maximum of $\bar{S}$ and an overestimation of the maximum ratio $\hat{S}/\bar{S}$ so that more stochastic patterns are marked to contain significant frequency components than expected by chance, c.f. numerical experiment in supplement section 6.5. The bias can only be substantially reduced by increasing the area over which a pattern is sampled. As the spatial extent of most patterns is not large, the test is biased. This has to be accounted for when evaluating the test result.

2.0.4. Arbitrarily pattern extents

The computation of the periodogram requires a pattern in a rectangular domain. Natural patterns usually do not extend over rectangular domains. They could be processed by clipping an aerial image to the largest rectangle fitting into the pattern. However, this is not satisfactory for striped patterns that grow in long and narrow valleys. In such cases the patterns are long, as many stripes occur along the valley, but the individual stripes are short, as their length is limited to width of the valley, c.f. patterns in Gandhi et al. (2018). Clipping an image to the interior extent of such a pattern results in a small image covering only a small part of the pattern. We therefore crop the image to the bounding box of the pattern, i.e. to the smallest rectangle fitting around the pattern. We exclude the area in the image not belonging to the pattern by masking, i.e. by setting the value of the pixels outside the area occupied by the pattern to the mean value of the pixels in the area occupied by the pattern. While this approach avoids clipping the pattern, the values of the periodogram cease to be statistically independent such that Eq. (6) does not hold any more. Therefore, we approximate the quantiles of the test statistic by Monte-Carlo-Simulation, c.f. supplement, section 6.2.

We verified the test, including the estimation of the non-flat spectral density and correction for multiple testing, with numerical experiments for Type-I and Type-II errors and found that it detects periodic components reliably even when the periodic component contributes a smaller fraction to the spatial variance of the pattern than the noise. We note that without the corrections, the number of false positives is unacceptably large, i.e. the test will misclassify almost all stochastic patterns as periodic. We provide a step-by-step instruction of the testing procedure in section 6.2 of the supplement.

2.0.5. Testing of average spectra

Several studies do not directly test the two-dimensional periodogram for significant frequency components. Instead, they test the periodogram after averaging along one-dimension (van de Koppel et al., 2005; Kefi et al., 2014). For isotropic (spotted) patterns, the periodogram is first transformed into radial coordinates before averaging (Couteron and Lejeune, 2001). Such tests can only determine if a pattern is regular or not, i.e. that the spectral density of the pattern is not flat, but not that a pattern contains periodic frequency components, as an average of the periodogram resembles a density estimate. Other studies test the autocorrelation function has a maximum that is significantly greater than zero (Weerman et al., 2010; van de Vijsel et al., 2020). Again, such tests can only determine if a pattern is regular or not, as for periodic patterns the amplitude of the autocorrelation is not just non-zero zero, but also does not decay. We note that both (van de Koppel et al., 2005) and van de Vijsel et al. (2020) consistently with our terminology describe their patterns as regular, and not as periodic.

3. Application of the test to regular environmental spatial patterns

We compiled a large global dataset of regular environmental spatial patterns due to the lack of a sufficient reference dataset. We included regions where regular spatial patterns were previously reported and regions with similar climate (Deblauwe et al., 2008; Borgogno et al., 2009). The regions consist of drylands in Australia, Africa and Northern America, and wetlands in central Africa. We manually identified patterns on the Google Satellite base map and delineated their spatial extent with polygons enclosing parts of patterns over which the patch size, spacing and orientation remain similar, c.f. Fig. 5b.

We automated the processing of the aerial images: First, the aerial image within the bounding box of a pattern is fetched and the area within the circumscribing polygon is masked. The spatial resolution of the image is adjusted between 4 m and 0.5 m depending on the spectrum. We keep the images in the pseudo-Mercator projection (EPSG:3857) provided by Google as it preserves angles and thus the

spatial structure over small areas. The scale distortion of the projection does not affect the spatial structure and remains limited since our dataset does not contain patterns in extreme latitudes. Images are converted to greyscale, with brighter areas corresponding to bare ground and darker areas to vegetation. Google Satellite imagery does not provide an infrared band for determining the NDVI, but it has a far higher spatial resolution compared to other publicly accessible global satellite imagery like Landsat which have near-infrared bands. Since we are interested in the spatial structure, not the total biomass, the superior spatial resolution is preferable over NDVI. The images then undergo quality control. Images where the dominant length scale cannot be clearly identified, images with patterns that are not strongly regular, or where the identified length scale is outside the range between 1 m and 500 m are discarded. The patterns are then grouped according to the world region they are located in.

At first, we inspect the autocorrelation structure and spectral density of the patterns. For this, we average the correlogram and periodogram in the direction perpendicular to stripes for anisotropic patterns and over equal angles after a transformation into polar coordinates for isotropic patterns. We normalize the axes by their characteristic scales, distances by λ_c and wavenumbers by k_c respectively, leading to graphs with unit-scale which can be directly compared and averaged. In polar coordinates, the cosines of the autocorrelation are transformed into Bessel-functions. The Bessel-functions oscillate with decaying amplitude even if the underlying pattern has periodic, i.e. hexagonal structure. This is because a periodic pattern only repeats along one of its axes of symmetry, while the transformation into radial coordinates averages over all directions. The transformation also slightly shifts the location of the first maximum of the autocorrelation. We compensate for the spurious decay of the radial autocorrelation by dividing it with the amplitude of the Bessel function, but we do not compensate for the shift, c.f. supplement 4.4. We then determine how well particular models fit the spectral density of the patterns, starting with the discrete spectrum of periodic patterns stemming from deterministic processes, as well as common unimodal densities stemming from stochastic processes, including the normal, log-normal and gamma-distributions. We fit the densities by minimizing the Hellinger distance HD, and measure the goodness of fit by the coefficient of determination, here defined as $R^2 = 1 - 2HD$, c.f. supplement section 5.4.

Finally, we test the spectra for significant frequency components with the amended procedure (Supplement section 6.2), adopting a significance level $\alpha = 0.05$. We compare the fraction P of patterns containing significant frequency components against the fraction of 5% expected for stochastic patterns, and assess the fraction of spatial variance contributed by significant components.

We determine the fractions by the total number of patterns per group, regardless of the spatial extent of each pattern, i.e. small and large patterns are equally weighted. Weighting the patterns by their surface area yields similar results. We limit the periodicity test to the frequency range which contributes most of the spatial variance, and exclude spurious low and high frequency components, c.f. Fig. 5c.

3.1. Fraction of patterns classified as periodic

We delineated more than 5514 anisotropic patterns, mostly striped, and more than 4817 isotropic patterns, primarily spotted. 2534 (46%) anisotropic and 3301 (69%) isotropic patterns passed the quality control and entered the analysis. The autocorrelations mark both the anisotropic and the isotropic patterns as clearly regular, as they oscillate at the characteristic wavelength λ_c (Fig. 6a_i, b_i). However, the autocorrelations show that the patterns are quite far from periodic as the oscillations are strongly damped, so that the first maximum R_c of the autocorrelation is far from 1, which is the expected value for periodic patterns. The spectral densities confirm the regularity of patterns, as all of them have a distinct maximum at the characteristic wavenumber k_c (Fig. 6a_{ii}, b_{ii}). The densities also confirm that the patterns are far from periodic as they consist of a wide lobe instead of narrow peaks. There are also no peaks superimposed on the lobed density, which would indicate the presence of hidden periodicities. The discrete density of a striped periodic or respectively a hexagonal periodic pattern does not fit the spectral density of most environmental spatial patterns well, with a median R^2 of −0.88 for anisotropic and −0.91 for isotropic patterns (Fig. 6a_{iii}, b_{iii}). In contrast, common unimodal parametric densities associated with stochastic processes fit the spectral density well, with median R^2 above 0.92 for anisotropic and above 0.95 for isotropic patterns.

To be certain that the patterns are not periodic, we apply the amended test. The median p-value of all isotropic patterns is 0.55, and of anisotropic patterns 0.49, indicating that most patterns are far from having a significant frequency component.

At a significance level of 0.05, 4.5% (113/2534) of the anisotropic patterns and 4.79% (158/3301) of the isotropic patterns have significant frequency components, close to the expected fraction of 5%. We note that it is not meaningful to determine a particular fraction of patterns with periodic frequency components when the patterns are stochastic, as the number of patterns with significant frequency components is close to the confidence level, which can be arbitrarily chosen. In our case, we chose the confidence level 0.05 for which we expect 5% of patterns to have significant frequency components. However, we can compare the fraction of patterns with significant frequency components against the expected fraction. If there would be patterns with periodic components originating from deterministic processes, the fraction of patterns with significant components would exceed the fraction expected for stochastic patterns. In our dataset, the fraction of patterns with significant frequency components ranges between 3% and 7% and does not considerably deviate from the expected value of 5% in any of the world regions (Fig. 7). There are thus not more patterns with significant frequency components than expected by chance. In addition, there is no world region where a sizeable fraction of patterns is classified as periodic. This result does not depend on the arbitrary threshold of $p = 0.05$. For the threshold $p = 0.01$ the result is similar: for 1.03% (46/2534) of the anisotropic patterns and 0.82% (28/3301) of the isotropic patterns the p-value falls below the threshold, compared to the expected fraction of 1%.

Beside the fraction of patterns with significant components, it is also relevant how much of the spatial variance of those patterns is explained by the significant frequency components. The fraction of spatial variance is identical to the fraction of spectral energy, i.e. the value of the spectral density of significant components. We find that significant frequency components only contribute a small amount of the total spectral energy of the respective patterns, on average only 0.26% for anisotropic and 0.58% for isotropic patterns at a 0.05 confidence level. For this reason, patterns with significant frequency components do not appear visually different, in particular not more regular than other patterns. For periodic patterns, the fraction of spectral energy contained in significant frequency components is considerably larger. For example, in the periodic plantations in Fig. 1, significant frequency components contain 49% of the spectral energy of the striped pattern and 30% of the spectral energy of the hexagonal pattern. For all patterns in our dataset the energy contained in the stochastic components, i.e. non-significant components, vastly exceeds the spectral energy contained in the significant frequency components identified by the periodicity test. Our dataset thus does not contain any patterns that can be classified as periodic.

While the overall result of our analysis is unambiguous, several factors might slightly influence the result. One factor is that patterns have been manually identified and delineated. Considering that our dataset comprises more than 8900 patterns on three continents, it is unlikely that testing other patterns or slightly changing the delineation results in a different conclusion. We note that our results also hold for an extended dataset including patterns in Asia and Southern America. We did not include the two continents in our analysis as to our

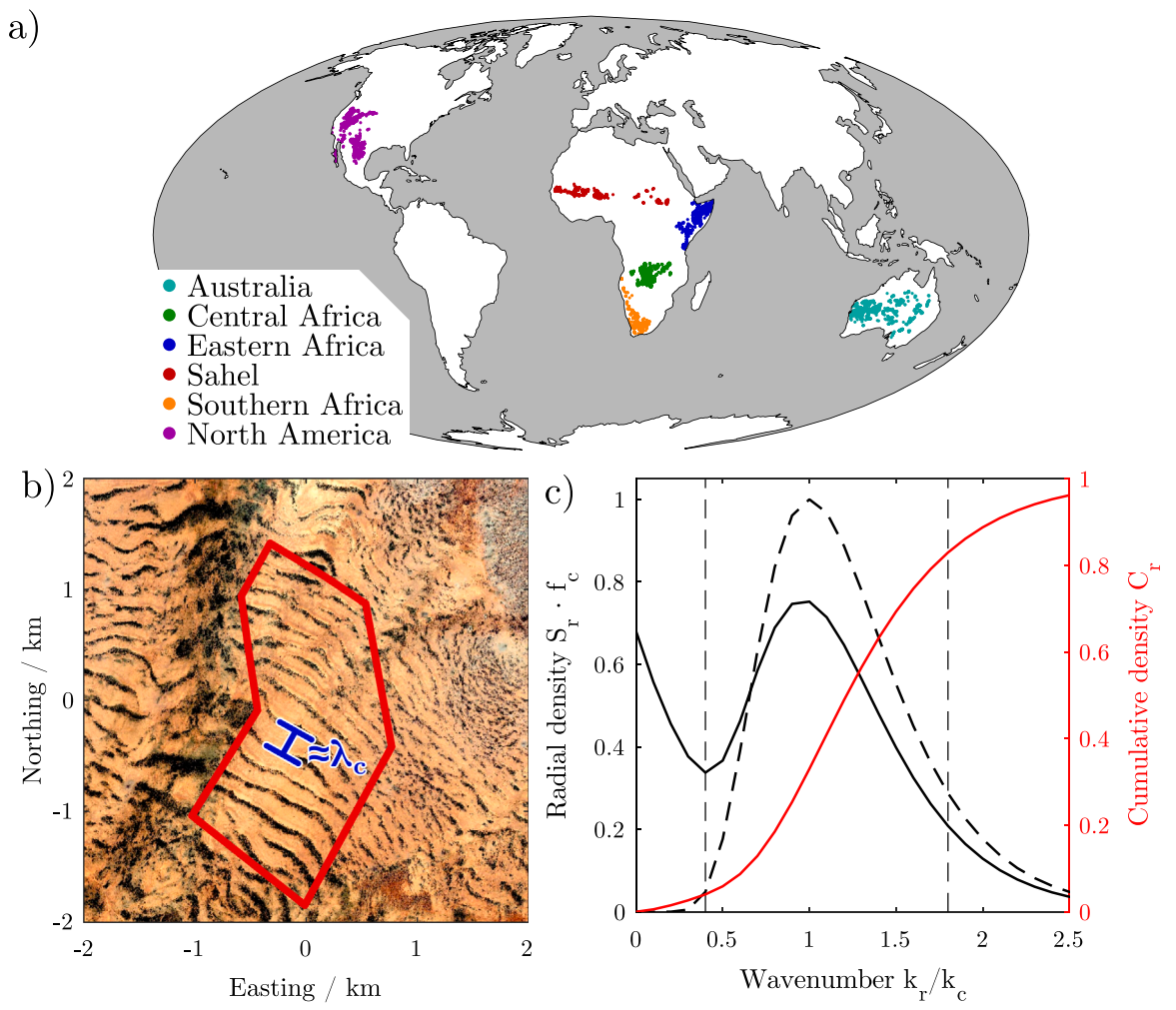

Fig. 5. (a) World regions where patterns were sampled. (b) An anisotropic dryland vegetation pattern in, near Burtinle, Somalia (47.9261°N 7.7911°N, Imagery 2023 Maxar Technologies and Google). The red polygon indicates the area masked for the periodicity test. The blue bar indicates the characteristic wavelength $\lambda_c = \frac{2\pi}{k_c}$. (c) Schematic radial spectral density S_r with spurious frequency components (solid) and after suppressing them (dashed). The dashed lines indicate the frequency range tested for periodic components, excluding spurious low and high frequency components (supplement section 5.3). We test for periodic components in the frequency range between the local minimum of the density S_r and the 80th-percentile of the cumulative distribution C_r (supplement section 3.4).

best knowledge there are no publications on regular patterns in the respective regions which would allow us to verify that those patterns indeed consist of vegetation. Another factor is that we retain only about half the patterns in the dataset after the quality check. This is because we only include highly regular patterns in the test. Including the less regular patterns does not change the result. It is also possible that some patterns in our dataset do not consist of vegetation, or did not form through self-organization. The fraction of such patterns is likely small, at least for the regions where the presence of regular vegetation patterns has already been established by previous studies. Another factor is that the p-value is sensitive to the smoothing radius chosen for estimating the density. A wider smoothing radius introduces the aforementioned bias so that slightly more patterns are flagged to contain significant frequency components. However, this bias is not large, as long as the smoothing radius is chosen consistently, i.e. as long as the spectrum is not oversmoothed to become flat, c.f. supplement section 6.5.

4. Discussion and conclusion

To determine if regular vegetation patterns are periodic, we compile and analyse a large dataset of isotropic, mostly spotted, and anisotropic, mostly striped, patterns. We find that the spatial structure of the patterns is dissimilar to that of periodic patterns. The oscillation of the autocorrelation decays rapidly instead of remaining constant like that of periodic patterns. Correspondingly, the spectral density is continuous instead of discrete like that of periodic patterns. We also show that the lack of a periodic structure cannot be explained by a mere variation of patch size, distance between patches or added spatial noise. The statistical test reveals that no more patterns have significant frequency components than expected by chance, and that significant frequency components only explain a negligible part of the spatial variance of a pattern, in case of the few patterns which have significant frequency components at all. In other words, not even a small subset of patterns is periodic, i.e. forming predominantly through deterministic processes. We find that the autocorrelation and spectrum of environmental spatial patterns is similar to patterns originating from stochastic processes. Spatial patterns synthesized by simple stochastic processes (Fig. 2c_i,d_i) can also appear similar to regular environmental spatial patterns (Fig. 1a_i, b_i). We emphasize that the patterns generated by a stochastic process can be regular and random at the same time, as the state at each point is random but the spatial correlation between the points makes it regular.

Our findings suggest that it is not meaningful to consider regularity as a dichotomous property and to classify environmental spatial

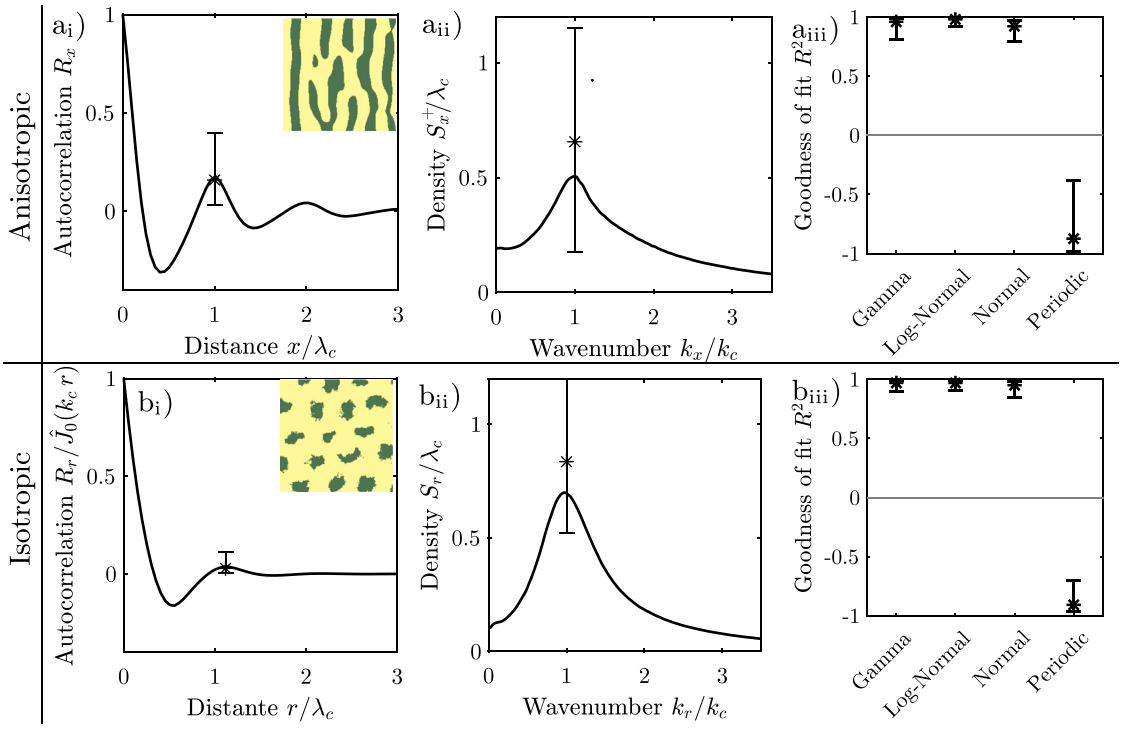

Fig. 6. (a_i) Autocorrelation and (a_{ii}) spectral density of anisotropic patterns in the direction perpendicular to the stripes, estimated by averaging over all patterns. Stars indicated the median and the end of sticks the 5th and 95th percentiles of the local maximum. (a_{iii}) Goodness of fit of parametric densities to the empirical spectral density in the direction perpendicular to the stripes. Stars indicated the median and the end of sticks the 5th and 95th percentiles of the fit to individual patterns. (b_i) Autocorrelation and (b_{ii}) spectral density of isotropic patterns in radial direction. The decay introduced to the autocorrelation by the transformation into polar coordinates is compensated for. (b_{iii}) Goodness of fit of parametric densities to the empirical radial spectral density.

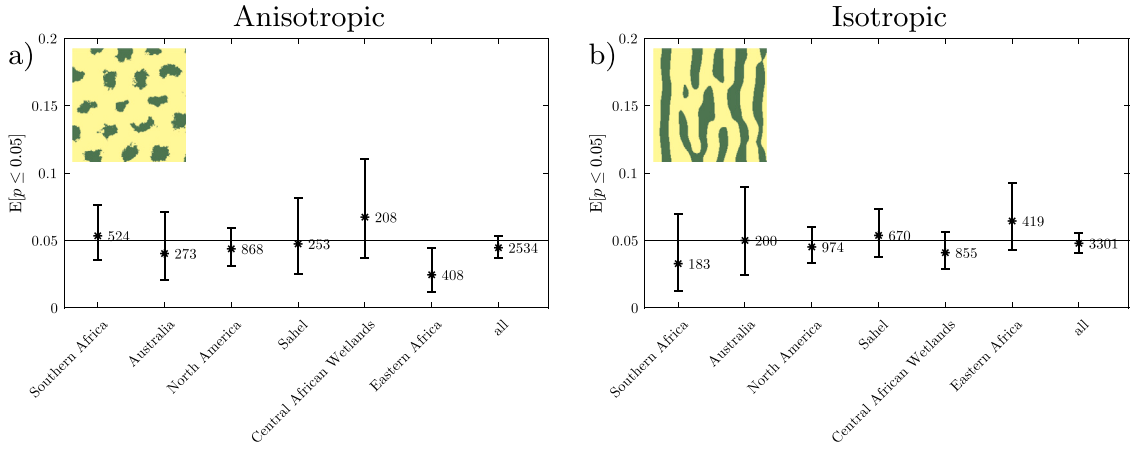

Fig. 7. Fraction P of (a) isotropic and (b) anisotropic patterns classified as periodic ($p \leq 0.05$). The numbers indicate the number of patterns in each region. The horizontal indicates the expected fraction of stochastic patterns which are classified as periodic by chance (5%). Error bars indicated the two sided 95% confidence interval determined with the Clopper–Pearson method (Ross, 2003).

patterns based on a periodicity test. Instead, regularity should be understood as a continuous variable, falling somewhere between the limit cases of irregular patterns, with no finite length scale on one end and periodic patterns on the other end. As regular spatial patterning is related to ecosystem functioning and resilience (Pringle et al., 2010; Liu et al., 2014; Bonachela et al., 2015; Rietkerk et al., 2021), there is a need for quantifying regularity beyond a binary classification. While the p-value of the statistical test takes continuous values between 0 and 1, its value for stochastic patterns is random irrespectively of their regularity. A different approach than statistical testing is thus required, which is in line with the general trend to move away from statistical testing (McShane et al., 2019; Wasserstein et al., 2019; Anderson et al., 2000). Any measure should appreciate the full spectrum of environmental spatial patterns in form of a probability distribution (Borgogno et al., 2009; Meron, 2015), i.e. go beyond analysing the characteristic wavelength.

The attribution of periodicity might stem partially from imprecise terminology, which in itself is trivial. However, it does have implications for modelling, as environmental spatial patterns are commonly studied with deterministic reaction–diffusion models which tend to generate periodic patterns (Klausmeier, 1999; Rietkerk and van de Koppel, 2008). Conventional reaction diffusion models are highly idealized and thus cannot be expected to reproduce all aspects in detail. Our findings indicate that deterministic models of vegetation patterns which tend to generate periodic patterns cannot reproduce the spatial structure of

regular vegetation patterns. This does not necessarily imply that the conclusions drawn from these models about ecosystem functionality and resilience are invalid. However, we think that care should be taken as the spatial structure has been suggested as an indicator of ecosystem health and function (Rietkerk et al., 2004; Yizhaq et al., 2005; Kéfi et al., 2010b).

Some deterministic systems can behave chaotically and generate non-periodic patterns (May, 1976; Devaney, 2018). While reaction–diffusion models commonly used for studying vegetation patterns could be modified to behave chaotically, this would require different parametrizations or processes than those which are currently understood to be physically plausible and relevant. Instead, we propose that noise, i.e. random spatial exogenous heterogeneities, influences the pattern formation, which turns the pattern formation from a deterministic into a stochastic process yielding regular patterns which fall short of being periodic. Conventional reaction diffusion models can be made more realistic by incorporating more biophysical processes in greater detail or accounting for temporal variation (Siteur et al., 2014; Gandhi et al., 2023). We advocate for not overlooking exogenous spatial heterogeneity here as deterministic models cannot reproduce the spatial structure of natural patterns, irrespectively of their complexity.

A few studies have demonstrated that noise can trigger the formation of regular patterns in ecosystems without scale-dependent feedbacks (Borgogno et al., 2009). While such stochastic models generate patterns which can appear more natural, they still do not mimic the underlying physical processes as the reaction–diffusion models do. We think that the key to reproducing natural patterns is to combine the deterministic and stochastic models, i.e. to integrate noise into reaction–diffusion models, rather than by superimposing it to model-generated patterns. Sources of spatio-temporal noise are numerous, and have in an ad-hoc manner been integrated in several studies, for example through the seed distribution (Pueyo et al., 2008; Realpe-Gomez et al., 2013), and extraneous spatial heterogeneities (Yizhaq et al., 2014; Yizhaq and Bel, 2016; Yizhaq et al., 2017; Castillo Vardaro et al., 2021). The role of spatio-temporal noise in pattern formation and its consequences for the functioning and resilience of pattern forming ecosystems needs to be studied in a more systematic way.

We present an analysis of regular dryland vegetation patterns here, as it is possible to compile a large dataset from satellite imagery. We note that we obtained similar results for a smaller set of regular patterns which are in other ecosystems including sea grass, mussel banks and algal mats. We therefore think that our results can be generalized to spatial biomass patterns which form through feedbacks with their underlying soil matrix. Patterns forming free of a supporting matrix, such as the honeycombs made by bees (Apis melifera), or patterns not in feedback with the supporting matrix, such as mega colonies of the great cormorant (Phalacrocorax carbo), or patterns that are too small to be affected by spatial heterogeneity, such as in Paleodictyon, can be periodic. This indicates that soil spatial heterogeneity likely plays a key role in the formation of environmental spatial patterns.

CRediT authorship contribution statement

Karl Kästner: Writing – review & editing, Writing – original draft, Visualization, Validation, Software, Resources, Methodology, Investigation, Formal analysis, Data curation, Conceptualization. **Roeland C. van de Vijsel:** Writing – review & editing. **Daniel Caviedes-Voullième:** Writing – review & editing. **Nanu T. Frechen:** Writing – review & editing. **Christoph Hinz:** Writing – review & editing.

Declaration of competing interest

The authors declare that they have no known competing financial interests or personal relationships that could have appeared to influence the work reported in this paper.

Acknowledgements

The authors thank Prof. Johan van de Koppel for his helpful comments during the review process.

Appendix A. Supplementary data

Supplementary material related to this article can be found online at https://doi.org/10.1016/j.catena.2024.108442.

Data availability

Computer scripts for fetching satellite images of the patterns from the Google maps server and for analysing them, geospatial input files and test result for each pattern are available at: https://github.com/karlkastner/environmental-spatial-patterns-periodicity-test. A snapshot of this repository which includes required library files is available at: https://zenodo.org/records/13695204. An interactive map of the dataset is available at: https://www.riverdolphin.xyz/vegetation-patterns.html (requires IPv6).

References

An, S.-I., Tziperman, E., Okumura, Y.M., Li, T., 2020. ENSO irregularity and asymmetry. El Niño South. Oscil. Chang. Clim. 153–172.

Anderson, D.R., Burnham, K.P., Thompson, W.L., 2000. Null hypothesis testing: Problems, prevalence, and an alternative. J. Wildl. Manage. 912–923.

Barbier, N., Bellot, J., Couteron, P., Wiegand, T., Grimm, V., Deblauwe, V., Biro, P., Mueller, E.N., 2014a. Assessment of patterns in ecogeomorphic systems. In: Patterns Land Degradation in Drylands: Understanding Self-Organised Ecogeomorphic Systems. pp. 247–264.

Barbier, N., Couteron, P., Deblauwe, V., 2014b. Case study of self-organized vegetation patterning in dryland regions of central africa. In: Patterns of Land Degradation in Drylands: Understanding Self-Organised Ecogeomorphic Systems. Springer, pp. 347–356.

Barbier, N., Couteron, P., Planchon, O., Diouf, A., 2010. Multiscale comparison of spatial patterns using two-dimensional cross-spectral analysis: Application to a semi-arid (gapped) landscape. Landsc. Ecol. 25 (6), 889–902.

Bastiaansen, R., Doelman, A., Eppinga, M.B., Rietkerk, M., 2020. The effect of climate change on the resilience of ecosystems with adaptive spatial pattern formation. Ecol. Lett. 23 (3), 414–429.

Boer, M., Puigdefábregas, J., 2005. Effects of spatially structured vegetation patterns on hillslope erosion in a semiarid mediterranean environment: A simulation study. Earth Surf. Process. Landf. J. Br. Geomorphol. Res. Group 30 (2), 149–167.

Bonachela, J.A., Pringle, R.M., Sheffer, E., Coverdale, T.C., Guyton, J.A., Caylor, K.K., Levin, S.A., Tarnita, C.E., 2015. Termite mounds can increase the robustness of dryland ecosystems to climatic change. Science 347 (6222), 651–655.

Borgogno, F., D'Odorico, P., Laio, F., Ridolfi, L., 2009. Mathematical models of vegetation pattern formation in ecohydrology. Rev. Geophys. 47 (1).

Castillo Vardaro, J.A., Bonachela, J.A., Baker, C.C., Pinsky, M.L., Doak, D.F., Pringle, R.M., Tarnita, C.E., 2021. Resource availability and heterogeneity shape the self-organisation of regular spatial patterning. Ecol. Lett. 24 (9), 1880–1891.

Couteron, P., 2001. Using spectral analysis to confront distributions of individual species with an overall periodic pattern in semi-arid vegetation. Plant Ecol. 156 (2), 229–243.

Couteron, P., 2002. Quantifying change in patterned semi-arid vegetation by Fourier analysis of digitized aerial photographs. Int. J. Remote Sens. 23 (17), 3407–3425.

Couteron, P., Barbier, N., Gautier, D., 2006. Textural ordination based on Fourier spectral decomposition: A method to analyze and compare landscape patterns. Landsc. Ecol. 21 (4), 555–567.

Couteron, P., Hunke, P., Bellot, J., Estrany, J., Martínez-Carreras, N., Mueller, E.N., Papanastasis, V.P., Parmenter, R.R., Wainwright, J., 2014. Characterizing patterns. In: Patterns of Land Degradation in Drylands. Springer, pp. 211–245.

Couteron, P., Lejeune, O., 2001. Periodic spotted patterns in semi-arid vegetation explained by a propagation-inhibition model. J. Ecol. 89 (4), 616–628.

Deblauwe, V., Barbier, N., Couteron, P., Lejeune, O., Bogaert, J., 2008. The global biogeography of semi-arid periodic vegetation patterns. Global Ecol. Biogeogr. 17 (6), 715–723.

Deblauwe, V., Couteron, P., Bogaert, J., Barbier, N., 2012. Determinants and dynamics of banded vegetation pattern migration in arid climates. Ecol. Monograph. 82 (1), 3–21.

Deblauwe, V., Couteron, P., Lejeune, O., Bogaert, J., Barbier, N., 2011. Environmental modulation of self-organized periodic vegetation patterns in sudan. Ecography 34 (6), 990–1001.
Devaney, R., 2018. An Introduction to Chaotic Dynamical Systems. CRC Press.
Ditlevsen, P.D., Kristensen, M.S., Andersen, K.K., 2005. The recurrence time of dansgaard–oeschger events and limits on the possible periodic component. J. Clim. 18 (14), 2594–2603.
Doodson, A.T., 1921. The harmonic development of the tide-generating potential. Proc. R. Soc. A 100 (704), 305–329.
Gandhi, P., Liu, L., Silber, M., 2023. A pulsed-precipitation model of dryland vegetation pattern formation. SIAM J. Appl. Dyn. Syst. 22 (2), 657–693.
Gandhi, P., Werner, L., Iams, S., Gowda, K., Silber, M., 2018. A topographic mechanism for arcing of dryland vegetation bands. J. R. Soc. Interface 15 (147), 20180 508.
Getzin, S., Wiegand, K., Wiegand, T., Yizhaq, H., von Hardenberg, J., Meron, E., 2015. Adopting a spatially explicit perspective to study the mysterious fairy circles of Namibia. Ecography 38 (1), 1–11.
Goehring, L., 2013. Pattern formation in the geosciences.
Jenkins, G.M., Priestley, M., 1957. The spectral analysis of time-series. J. R. Stat. Soc. Ser. B Stat. Methodol. 19 (1), 1–12.
Johnston, S., Gous, R., 2007. A mechanistic, stochastic, population model of egg production. Br. Poult. Sci. 48 (2), 224–232.
Kéfi, S., Alados, C.L., Chaves, R., Pueyo, Y., Rietkerk, M., 2010a. Is the patch size distribution of vegetation a suitable indicator of desertification processes? Comment.
Kéfi, S., Eppinga, M.B., de Ruiter, P.C., Rietkerk, M., 2010b. Bistability and regular spatial patterns in arid ecosystems. Theor. Ecol. 3 (4), 257–269.
Kefi, S., Guttal, V., Brock, W.A., Carpenter, S.R., Ellison, A.M., Livina, V.N., Seekell, D.A., Scheffer, M., van Nes, E.H., Dakos, V., 2014. Early warning signals of ecological transitions: Methods for spatial patterns. PLoS One 9 (3), e92, 097.
Kéfi, S., Rietkerk, M., Alados, C.L., Pueyo, Y., Papanastasis, V.P., ElAich, A., De Ruiter, P.C., 2007. Spatial vegetation patterns and imminent desertification in Mediterranean arid ecosystems. Nature 449 (7159), 213–217.
Klausmeier, C.A., 1999. Regular and irregular patterns in semiarid vegetation. Science 284 (5421), 1826–1828.
Kletter, A.Y., Von Hardenberg, J., Meron, E., 2012. Ostwald ripening in dryland vegetation. Commun. Pure Appl. Anal. 11, 261–273.
Kondo, S., Miura, T., 2010. Reaction–diffusion model as a framework for understanding biological pattern formation. Science 329 (5999), 1616–1620.
Kovačević, B., Djurović, Ž., 2008. Fundamentals of Stochastic Signals, Systems and Estimation Theory with Worked Examples. Springer.
Lejeune, O., Tlidi, M., Lefever, R., 2004. Vegetation spots and stripes: Dissipative structures in arid landscapes. Int. J. Quantum Chem. 98 (2), 261–271.
Li, T.-H., 2013. Time Series with Mixed Spectra. CRC Press.
Liu, Q.-X., Herman, P.M., Mooij, W.M., Huisman, J., Scheffer, M., Olff, H., van de Koppel, J., 2014. Pattern formation at multiple spatial scales drives the resilience of mussel bed ecosystems. Nature Commun. 5 (1), 1–7.
Maestre, F.T., Eldridge, D.J., Soliveres, S., Kéfi, S., Delgado-Baquerizo, M., Bowker, M.A., García-Palacios, P., Gaitán, J., Gallardo, A., Lázaro, R., et al., 2016. Structure and functioning of dryland ecosystems in a changing world. Annu. Rev. Ecol. Evol. Syst. 47, 215–237.
Mander, L., Dekker, S.C., Li, M., Mio, W., Punyasena, S.W., Lenton, T.M., 2017. A morphometric analysis of vegetation patterns in dryland ecosystems. R. Soc. Open Sci. 4 (2), 160, 443.
May, R.M., 1976. Simple mathematical models with very complicated dynamics. Nature 261 (5560), 459–467.
McShane, B.B., Gal, D., Gelman, A., Robert, C., Tackett, J.L., 2019. Abandon statistical significance. Amer. Statist. 73 (sup1), 235–245.
Meron, E., 1992. Pattern formation in excitable media. Phys. Rep. 218 (1), 1–66.
Meron, E., 2015. Nonlinear Physics of Ecosystems. CRC Press, Boca Raton, FL.
Messaoudi, M., Clerc, M.G., Berríos-Caro, E., Pinto-Ramos, D., Khaffou, M., Makhoute, A., Tlidi, M., 2020. Patchy landscapes in arid environments: Nonlinear analysis of the interaction-redistribution model. Chaos 30 (9).
Moreno-de Las Heras, M., Saco, P.M., Willgoose, G.R., Tongway, D.J., 2011. Assessing landscape structure and pattern fragmentation in semiarid ecosystems using patch-size distributions. Ecol. Appl. 21 (7), 2793–2805.
Mugglestone, M.A., Renshaw, E., 1998. Detection of geological lineations on aerial photographs using two-dimensional spectral analysis. Comput. Geosci. 24 (8), 771–784.
Murray, J.D., 2002. Mathematical Biology I: An Introduction. Springer.
Okayasu, T., Aizawa, Y., 2001. Systematic analysis of periodic vegetation patterns. Progr. Theoret. Phys. 106 (4), 705–720.
Ouyang, Q., Swinney, H.L., 1991. Transition from a uniform state to hexagonal and striped turing patterns. Nature 352 (6336), 610–612.
Parker, B.B., 2007. Tidal analysis and prediction.
Parzen, E., 1957. On consistent estimates of the spectrum of a stationary time series. Ann. Math. Stat. 329–348.
Pascual, M., Guichard, F., 2005. Criticality and disturbance in spatial ecological systems. Trends Ecol. Evol. 20 (2), 88–95.
Penny, G.G., Daniels, K.E., Thompson, S.E., 2013. Local properties of patterned vegetation: Quantifying endogenous and exogenous effects. Phil. Trans. R. Soc. A 371 (2004), 20120 359.
Percival, D.B., Walden, A.T., et al., 1993. Spectral Analysis for Physical Applications. Cambridge University Press.
Pielou, E., 1964. The spatial pattern of two-phase patchworks of vegetation. Biometrics 156–167.
Pringle, R.M., Doak, D.F., Brody, A.K., Jocqué, R., Palmer, T.M., 2010. Spatial pattern enhances ecosystem functioning in an African savanna. PLoS Biol. 8 (5), e1000, 377.
Pueyo, Y., Kéfi, S., Alados, C., Rietkerk, M., 2008. Dispersal strategies and spatial organization of vegetation in arid ecosystems. Oikos 117 (10), 1522–1532.
Realpe-Gomez, J., Baudena, M., Galla, T., McKane, A.J., Rietkerk, M., 2013. Demographic noise and resilience in a semi-arid ecosystem model. Ecol. Complex. 15, 97–108.
Renshaw, E., Ford, E., 1984. The description of spatial pattern using two-dimensional spectral analysis. Vegetatio 56 (2), 75–85.
Rietkerk, M., Bastiaansen, R., Banerjee, S., van de Koppel, J., Baudena, M., Doelman, A., 2021. Evasion of tipping in complex systems through spatial pattern formation. Science 374 (6564), eabj0359.
Rietkerk, M., Boerlijst, M.C., van Langevelde, F., Hille Ris Lambers, R., van de Koppel, J., Kumar, L., Prins, H.H., de Roos, A.M., 2002. Self-organization of vegetation in arid ecosystems. Amer. Nat. 160 (4), 524–530.
Rietkerk, M., Dekker, S.C., Ruiter, P.C. De, van de Koppel, J., 2004. Self-organized patchiness and catastrophic shifts in ecosystems. Science 305 (5692), 1926–1929.
Rietkerk, M., van de Koppel, J., 2008. Regular pattern formation in real ecosystems. Trends Ecol. Evol. 23 (3), 169–175.
Roitberg, E., Shoshany, M., 2017. Can spatial patterns along climatic gradients predict ecosystem responses to climate change? Experimenting with reaction–diffusion simulations. PLoS One 12 (4), e0174, 942.
Ross, T.D., 2003. Accurate confidence intervals for binomial proportion and Poisson rate estimation. Comput. Biol. Med. 33 (6), 509–531.
Sankaran, S., Majumder, S., Viswanathan, A., Guttal, V., 2019. Clustering and correlations: Inferring resilience from spatial patterns in ecosystems. Methods Ecol. Evol. 10 (12), 2079–2089.
Scheffer, M., Bascompte, J., Brock, W.A., Brovkin, V., Carpenter, S.R., Dakos, V., Held, H., van Nes, E.H., Rietkerk, M., Sugihara, G., 2009. Early-warning signals for critical transitions. Nature 461 (7260), 53–59.
Sheffer, E., von Hardenberg, J., Yizhaq, H., Shachak, M., Meron, E., 2013. Emerged or imposed: A theory on the role of physical templates and self-organisation for vegetation patchiness. Ecol. Lett. 16 (2), 127–139.
Siero, E., Doelman, A., Eppinga, M., Rademacher, J.D., Rietkerk, M., Siteur, K., 2015. Striped pattern selection by advective reaction–diffusion systems: Resilience of banded vegetation on slopes. Chaos 25 (3), 036 411.
Siteur, K., Liu, Q.-X., Rottschäfer, V., van der Heide, T., Rietkerk, M., Doelman, A., Boström, C., van de Koppel, J., 2023. Phase-separation physics underlies new theory for the resilience of patchy ecosystems. Proc. Natl. Acad. Sci. 120 (2), e2202683, 120.
Siteur, K., Siero, E., Eppinga, M.B., Rademacher, J.D., Doelman, A., Rietkerk, M., 2014. Beyond turing: The response of patterned ecosystems to environmental change. Ecol. Complex. 20, 81–96.
Stone, L., Saparin, P.I., Huppert, A., Price, C., 1998. El Nino chaos: The role of noise and stochastic resonance on the ENSO cycle. Geophys. Res. Lett. 25 (2), 175–178.
Thomas, D., 1973. Multiple comparisons among means—a review. J. R. Stat. Soc. Ser. D: Stat. 22 (1), 16–42.
Tlidi, M., Berríos-Caro, E., Pinto-Ramo, D., Vladimirov, A., Clerc, M.G., 2020. Interaction between vegetation patches and gaps: A self-organized response to water scarcity. Physica D 414, 132, 708.
van de Koppel, J., Rietkerk, M., Dankers, N., Herman, P.M., 2005. Scale-dependent feedback and regular spatial patterns in young mussel beds. Amer. Nat. 165 (3), E66–E77.
van de Vijsel, R.C., van Belzen, J., Bouma, T.J., van der Wal, D., Cusseddu, V., Purkis, S.J., Rietkerk, M., van de Koppel, J., 2020. Estuarine biofilm patterns: Modern analogues for Precambrian self-organization. Earth Surf. Process. Landf. 45 (5), 1141–1154.
van Kampen, N.G., 1976. Stochastic differential equations. Phys. Rep. 24 (3), 171–228.
von Hardenberg, J., Kletter, A.Y., Yizhaq, H., Nathan, J., Meron, E., 2010. Periodic versus scale-free patterns in dryland vegetation. Proc. R. Soc. B: Biol. Sci. 277 (1688), 1771–1776.
Wang, C., Wang, H., Yuan, S., 2023. Precipitation governing vegetation patterns in an arid or semi-arid environment. J. Math. Biol. 87 (1), 22.
Wasserstein, R.L., Schirm, A.L., Lazar, N.A., 2019. Moving to a world beyond $p < 0.05$.

Weerman, E., van Belzen, J., Rietkerk, M., Temmerman, S., Kéfi, S., Herman, P., van de Koppel, J., 2012. Changes in diatom patch-size distribution and degradation in a spatially self-organized intertidal mudflat ecosystem. Ecology 93 (3), 608–618.
Weerman, E.J., van de Koppel, J., Eppinga, M.B., Montserrat, F., Liu, Q.-X., Herman, P.M., 2010. Spatial self-organization on intertidal mudflats through biophysical stress divergence. Amer. Nat. 176 (1), E15–E32.
Yizhaq, H., Bel, G., 2016. Effects of quenched disorder on critical transitions in pattern-forming systems. New J. Phys. 18 (2), 023 004.
Yizhaq, H., Gilad, E., Meron, E., 2005. Banded vegetation: Biological productivity and resilience. Phys. A 356 (1), 139–144.
Yizhaq, H., Sela, S., Svoray, T., Assouline, S., Bel, G., 2014. Effects of heterogeneous soil–water diffusivity on vegetation pattern formation. Water Resour. Res. 50 (7), 5743–5758.
Yizhaq, H., Stavi, I., Shachak, M., Bel, G., 2017. Geodiversity increases ecosystem durability to prolonged droughts. Ecol. Complex. 31, 96–103.
Zelnik, Y.R., Kinast, S., Yizhaq, H., Bel, G., Meron, E., 2013. Regime shifts in models of dryland vegetation. Phil. Trans. R. Soc. A 371 (2004), 20120 358.
Zelnik, Y.R., Meron, E., Bel, G., 2015. Gradual regime shifts in fairy circles. Proc. Natl. Acad. Sci. 112 (40), 12 327–12, 331.